3.4. Conformational Analysis With Geometric & Experimental Constraints

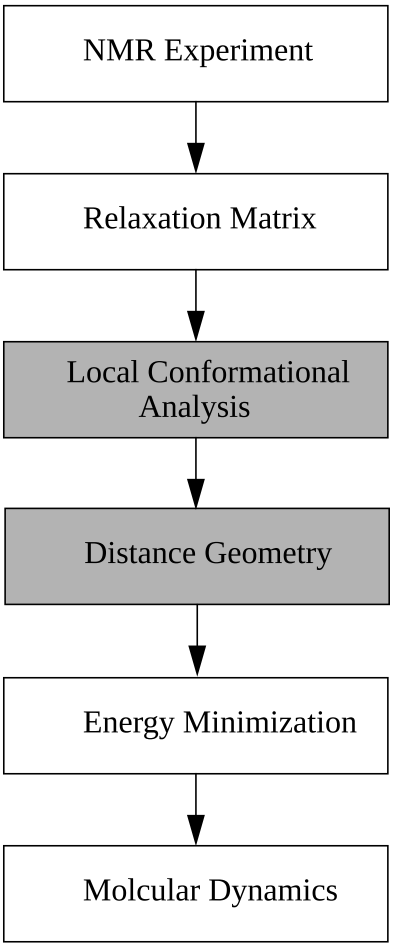

The problem of defining a biomolecule structure on the basis of pure experimental information can be divided into two sub-processes:

- calculation of conformations for the individual building blocks (amino acids/nucleotides);
- determination of the overall fold (for the complete biopolymer sequence).

The first step can be achieved by a local conformational analysis which mainly takes into consideration all **intra**-residual restraints. Evaluations result in a decription of allowed ranges for the torsion angles of fragments. From this locally constrained conformational space the starting structures can be randomly chosen.

In the second step distance geometry calculations are performed taking these starting structures. **Inter**-residual restraints are added to the data and the result is the definition of the secondary and tertiary structure of the whole biomolecule.

3.4.1. Local Conformational Analysis (LCA)

Several programs for an unbiased screening of the local constraints exist which produce stereospecific assignments and allowed regions in the local conformational space, the so-called angle constraints. These programs (HABAS, ANGLESEARCH) are mainly designed for proteins.

Another feature is the comparison of the experimentally obtained chemical shifts with the chemical shift index (CSI; Wishart & Sykes, 1994). This ‘library’ includes data for C^{α}, C^{β}, C’ and H^{α} atoms of every amino acid. If a series of index values specific for a secondary structure element is recognized, broad angle constraint ranges for the ψ and ϕ torsions according to the Ramachandran plot can be added to the input data for a DG run

An example for the CSI method is shown. The table lists the library entries for the H^{α} chemical shifts. The figure displays the results after the filtering process (see Protocol below) for Thioredoxin (Wishart & Sykes (1994) Biochemistry 31, 1647-1651).

residue	α-^{1}H range (ppm)	residue	α-^{1}H range (ppm)
Ala	4.35 ± 0.10	Met	4.52 ± 0.10
Cys	4.65 ± 0.10	Asn	4.75 ± 0.10
Asp	4.76 ± 0.10	Pro	4.44 ± 0.10
Glu	4.29 ± 0.10	Gln	4.37 ± 0.10
Phe	4.66 ± 0.10	Arg	4.38 ± 0.10
Gly	3.97 ± 0.10	Ser	4.50 ± 0.10
His	4.63 ± 0.10	Thr	4.35 ± 0.10
Ile	3.95 ± 0.10	Val	3.95 ± 0.10
Lys	4.36 ± 0.10	Trp	4.70 ± 0.10
Leu	4.17 ± 0.10	Tyr	4.60 ± 0.10

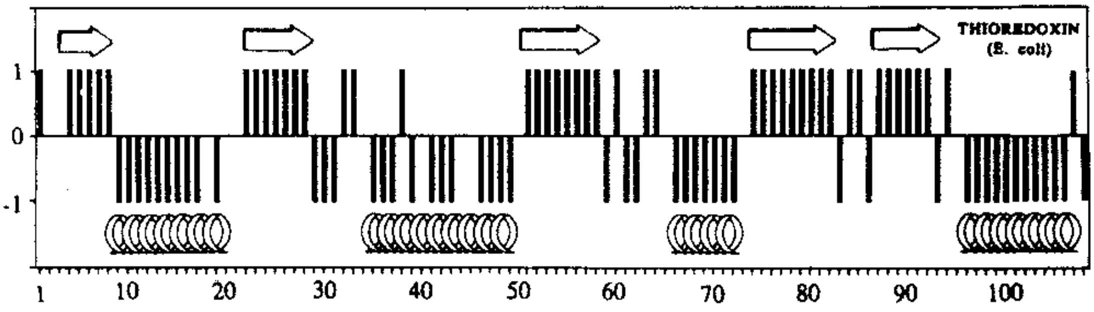

Protocol of the Chemical Shift Index for proteins:

1. Obtain sequential assignment for H^{α}, C^{α}, C’, C^{β} or N’.

2. Classify according to the CSI-tables:

a. if the experimental shift is greater than the tabled range, mark residue with +1;

b. if the experimental shift is lower than the tabled range, mark residue with -1;

c. if the experimental shift is within the tabled range, mark residue with 0.

3. Convert to secondary structure elements according to the following rules:

a. any group of four “-1’s” not interrupted by a “1” is a helix;

b. any group of three “1’s” not interrupted by a “-1” is a strand;

c. any other combination is a coil;

d. the local density of “-1’s” and “1’s” measured for a window of four to five residues has to exceed 70% for definition of a structured element;

e. termination points of helices or strands can be recognized by the first appearance of an opposite sign or two consecutive zeros in the CSI.

4. Be aware of the following critical questions:

- *the results depend on the quality of the acquired chemical shift index*;
- the procedure works best for NMR conditions of pH 3.0-8.0 and 15-50^{o}C;
- applications to proteins with paramagnetic centers will produce incorrect results;
- for glycine, the average shift of the two nonequivalent α-protons should be used;
- this empirical procedure has “only” an accuracy of up to 95%;
- there is no intention to replace the rigorous methods in NMR structure determination.

Translation of predicted Secondary Structure Elements into angle constraints:

Secondary structure elements are connectable to ϕ-, ψ-torsion angle ranges by Ramachandran maps but the regions for various amino acids differ according to the side chain steric volume and other conformational parameters.
As a first approximation an increased standard range can be used:
- α-helix: ϕ = -150 to -30, ψ = -90 to 30;
- β-sheet: ϕ = -180 to -30, ψ = 40 to 190.

Distance informations are introduced either by steric considerations or by upper- and lower-limit files:

Every atom r has an assigned repulsive core radius. Thus, in general, for each distance relation the sum of van-der-Waals radii define the **lower limit**. A violation exists, if

$$d_{actual} < r_A + r_B \ .$$

Under some circumstances it might be helpful to introduce further restrictions via lower limits. E.g. if one is sure, that a certain NOE cross peak is not to be observed, this ‘non-NOE’ can be converted in a lower distance > 7 Å.

The discussion of the ISPA method has shown that distance constraints often have a considerable error even if an intensity error is related to a distance error by the 6th root. In order to deal with this inaccuracy several possibilities exist for the introduction of **upper limits**:

- all interproton distances are assigned to a upper bound of 5-6 Å (reasonable for long mixing times at large molecules);
- subdivision into 3 to 4 distance classes/intensity classes with strong = 1.8-2.8 Å, medium = 1.8-3.3 Å and weak = 1.8-5.0 Å;
- treatment using the exact distances derived from relaxation matrix calculations.

LCA is essentially a grid search in which every torsion angle within a predefined fragment is systematically varied against all other torsions. Hence, the **number of torsions** t considered defines the dimensionality of the mathematical problem and the **grid search step width** w influences the computational effort.

The **total number of variations** v obeys the formula: $v = w^t$.

A grid width of 10° leads to 36 adjustment steps for each angle and a fragment of 5 torsions therefore needs 36^5 = 60.466.176 single calculation steps!

After each variation the experimental data with exclusion of all medium-range and long-range NOE’s are scanned. The HABAS (Güntert et al., (1989) J.Am.Chem.Soc. 111, 3997-4004) approach takes into account the intraresidual distances $d_{N\alpha}$, $d_{N\beta}$, $d_{N\gamma}$ ... and the sequential distances d_{NN}, $d_{\beta N}$ etc. In case of a contradiction between expected and experimental distance or J-coupling value the actual conformer is rejected. Stereospecific assignment is performed by two grid searches of the same fragment with exchanged proton assignment. The number of conformations fulfilling all experimental constraints is computed. An unambiguous assignment exists if $n_{H\beta 2/H\beta 3} = 0$ while $n_{H\beta 3/H\beta 2} > 0$.

Conversion of J-coupling constants into dihedral angle ranges

Consider the parametrized $^3J_{PH3'}/^3J_{PC2'}/^3J_{PC4'}$-coupling constants describing the ε-torsion in a nucleic acids fragment. The plot shows the intersection principle for the determination of allowed conformation and torsion angle constraints. If a torsion is defined by multiple J-couplings (e.g. 8.0 Hz/2.1 Hz/9.8 Hz, respectively) only those conformations are accepted which fulfill all given J-coupling data. Here, only in one area of the ε-torsion space an intersection of all three curves occur. Therefore, the angle rotation can be restricted to a range between 200 and 220° (white bar on the top of the plot). The intersection between two ranges near 0° is not accepted (black bar).

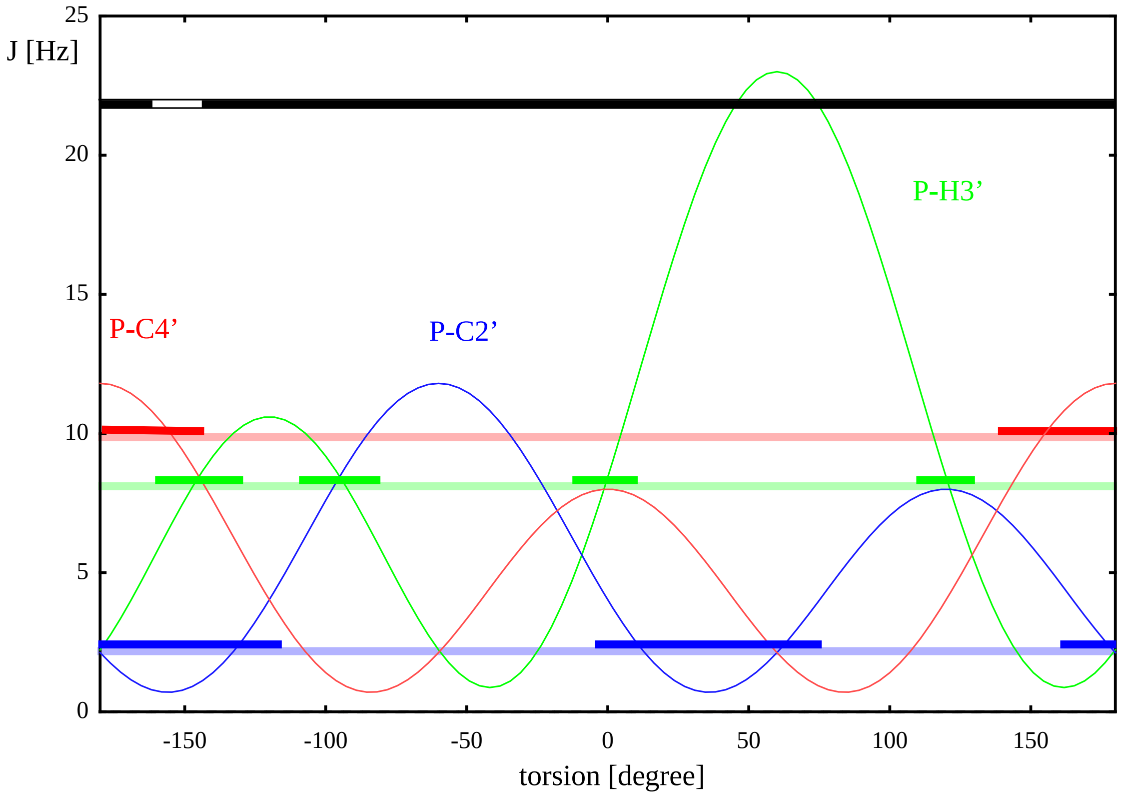

Example for a DIANA angle constraint file:

```
#                                  -180  -120   -60     0    60   120   180
#                                     |     |     |     |     |     |     |
   2 RGUA  BETA   -175.0    45.0 #    .++   .     .    ++   + .     .
   2 RGUA  NU1    -185.0    45.0 #    +++++ .     .     +++++ .     .
   2 RGUA  EPSI   -160.0  -140.0 #    . +++ .     .     .     .     .
```

The dihedral angle range may be further limited by steric interactions or upper/lower limit violations.

3.4.2. Distance Geometry (DG)

Distance geometry calculations may be performed in the metric matrix space or in the dihedral angle space.

Metric matrix DG, DGEOM (Crippen, 1977; Havel et al., 1983)

- All distance constraints are used to build upper and lower **distance bound matrices** for each proton pair. Upper bounds not known are set to a value greater than the molecules size, unknown lower bounds are set to the sum of van-der-Waals radii.
- The conformational space is then reduced by ‘bounds **smoothing**’, where lower bounds are increased and upper bounds are lowered by application of the triangle inequality. This means that for three atoms the furthest distance a, b is obtained, when all atoms are colinear and c lies in between a and b.

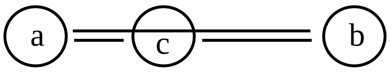

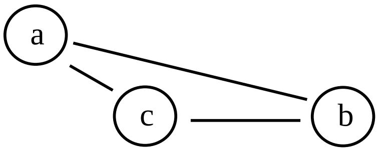

  Therefore, the upper bounds follow: $u_{ab} \le u_{ac} + u_{cb}$

  If u_{ab} is greater than $u_{ac} + u_{cb}$ this value can be decreased to $u_{ac} + u_{cb}$. This procedure is done for all tripels of atoms. Similarily, the lower limits can be smoothed, but this process requires knowledge about one upper bound per tripel. Inability to solve the inequalities indicates problems with the input constraints.
- In the next step, **trial distances** are chosen from a random distribution or distribution function. Since this step turned out to be critical for the success, one should use a distribution which weights shorter distances stronger. Otherwise, structures tend to occupy extended conformations.
- **Embedding** is the conversion of distances into coordinates by calculating the metric matrix via the cosine rule. The atomic coordinates $\mathbf{c}_i$ in one dimension of the cartesian space are related to the eigenvalues λ_i and eigenvectors $\mathbf{w}_i$ by

$$c_i = \sqrt{\lambda_i} \cdot \boldsymbol{w}_i$$

  The roots of the eigenvalues are the principal moments of the molecule with respect to the coordinate origin of the molecule at the molecular centroid. The eigenvectors are the distributions of the atoms along the axes.

  If a non-zero eigenvalue of this square matrix is found, the coordinates are known. Since more than three solutions exist, the multidimensional coordinate set is transferred into a 3D set by selecting the largest eigenvalue.
- The selection of solutions for the eigenvalue problem is rather arbitrary so that the resulting structures will not meet all boundary conditions. To compensate this gap, an **optimization** for lowest error between distances and desired boundary conditions by manipulation of the coordinates is employed using the cycle:

  - Calulation of the error function;
  - Calculation of a gradient;
  - Changes in coordinates by a arbitrary step;
  - Reevaluation of the error function;

- Acceptance and new cycle, if new error is less.
Distances and local chiral centers are considered in the optimization phase.

The computational effort for metric matrix DG is very high since in the smoothing step the CPU time is proportional to N^3, where N is the number of atoms. Also storage of the coordinates set requires more disk space since for atom position is notated by 3 coordinates.

Torsion space DG, DIANA (Braun & Go, 1985; Güntert et al., 1991)
In contrast to modifying the coordinates of a molecule this procedure is based on variations in torsion angles. A variable target function is employed to compare the quality of calculated conformers.

- Identification of irrelevant and too restrictive constraints.
  Experimental data is ***irrelevant*** and will be removed from the input file, if:
  1. a lower limit is smaller than the steric limit;
  2. a distance is independent of the conformation (e.g. fixed geminal distances);
  3. no conformation will violate the limit (b >= A + B).

  Case 3. can only be checked for one-angle dependent distances since a mathematical relation exists:

$$A - B \leq \left|r_A - r_B\right|^2 \leq A + B$$

$$A = \left|d_A\right|^2 + \left|d_B\right|^2 - 2(e_A d_A)(e_A d_B)$$

$$B = \sqrt{\left[d_A^2 - (e_A d_A)^2\right]\left[d_A^2 - (e_A d_B)^2\right]}$$

  e_A is the unit vector along the rotatable bond.
  From these equations also ***too restrictive data*** can be derived, then b < A - B .
- The checks for steric overlap -in principle- have to be performed after each evaluation step for all atom pairs and becomes very time consuming (1.000 atoms => 500.000 atom pairs). In order to reduce the effort it is sufficient to store all pairs with reasonable small distances (30.000 pairs) in a nonbonded-pair list which is updated after several calculation steps. This list contains:
  - an invariant part with itra-residual and sequential distances;
  - a part to be updated after e.g. 50 iterations or a torsion change of 10° in which all atom pairs within a 3.2 Å radius around one atom are stored.
- The calculation starts with a random conformation.
- The target function is evaluated by summation of all contributions from violated constraints.
- The target function is optimized by a conjugate gradient minimization in several steps taking into account
  - intra-residual distances first;
  - short-range constraints;
  - medium-range contraints;

- long-range constraints.

This division of the minimization problem into several steps prevents the process to be captured in a local minimum.

The minimizer stops if the gradient reaches a threshold value or the maximal number of evaluations is reached.

The variable target function is defined by:

$$T = \sum_{c = u, l, v} w_c \cdot \sum_{\alpha, \beta \in I_c} \left[\Theta_c \left(\frac{d_{\alpha\beta}^2 - b_{\alpha\beta}^2}{2 b_{\alpha\beta}} \right) \right]^2 + w_a \sum_{\alpha \in I_a} \left[1 - \frac{1}{2} \left(\frac{\Delta_a}{\Gamma_a} \right)^2 \right] \Delta_a^2$$

with

w_c, w_a : weighting factors for distance and angle constraints
$d_{\alpha\beta}$: distance between two atoms
$b_{\alpha\beta}$: distance limit between the two atoms
Δ_a : violation of the dihedral angle
Γ_a : half width of the forbidden dihedral angle interval
c : consists of contributions for upper (u), lower (l) and steric limits (v)

The following figure (Güntert et al., 1991) explains the influence of the minimization level on the structure definition. The minimization level corresponds to the number of residues between which a distance constraint is considered in the current optimization step.

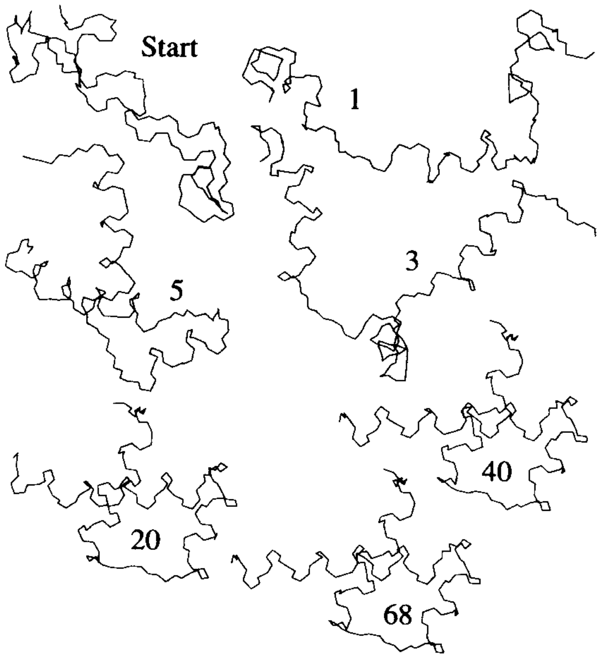

Intermediate structures during the minimization with the program DIANA of the *Antp*$(C39 \rightarrow S)$ homeodomain conformation with the smallest final target function value among the 250 conformations that were calculated. The backbone atoms of residues 7 to 59 of the random start conformation, and of the conformations at the end of the minimization levels $L = 1, 3, 5, 20, 40$ and 68 are shown.

The efficiency of the DIANA calculations is improved by use of **redundant angle constraints** (REDAC; Güntert and Wüthrich, 1991). The flow chart compares the direct and REDAC-cycle approach. Difference in the two calculations are additional steps providing a partial feedback of structural information from all conformers that were calculated. Structures with low constraint violations in a particular residue and its two neighbours are stored. If 20% of the maximal number of calculated conformers are found to be acceptable, from these new dihedral angle constraints are evaluated by taking the two extreme values in this group of molecules as upper and lower range limit. A second test assures that the new constraint is meaningful. If the assigned torsion interval is larger than 270°, the constraint is discarded, otherwise added as input for a new structure calculation in step B.

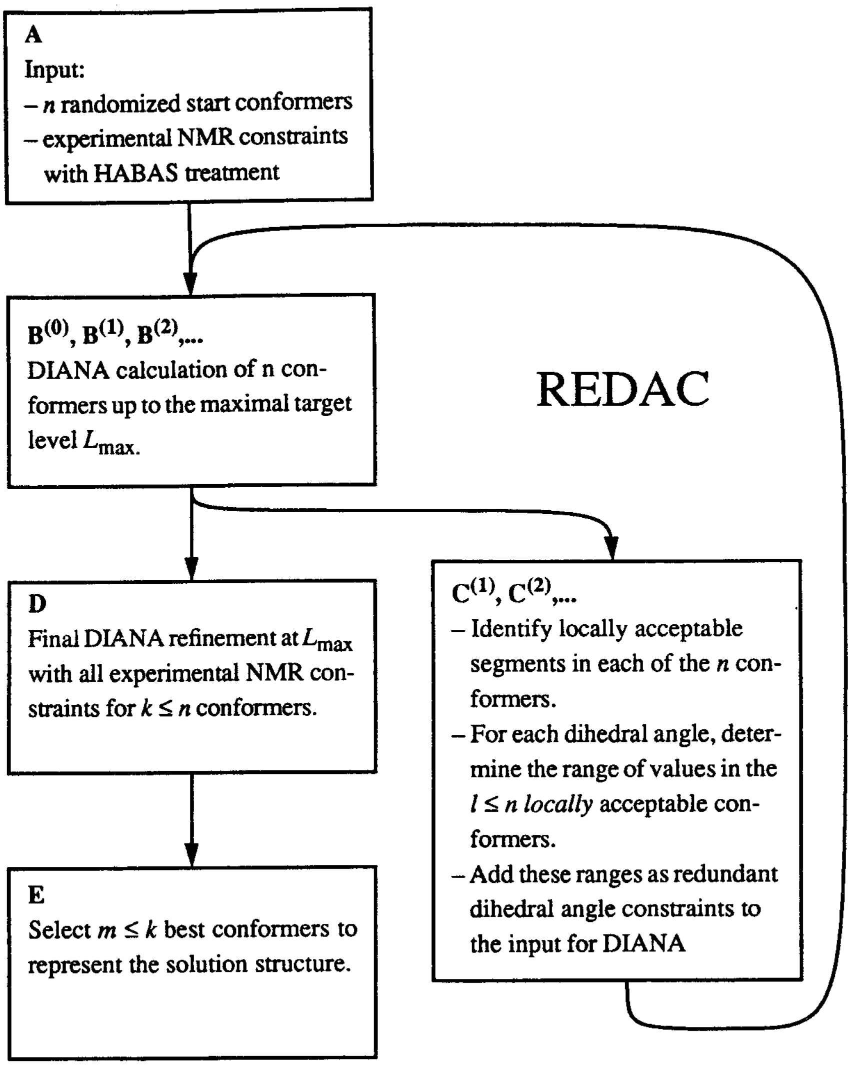

Flowchart outlining the course of a protein structure calculation with the program DIANA using either the 'direct' way (A-$B^{(0)}$-D-E) or REDAC (A-$B^{(0)}$-[$C^{(1)}$-$B^{(1)}$-...]-D-E). Typically, the number of REDAC-cycles is 1 or 2.

The table depicts the improvement using the REDAC cycle for three different molecules. n gives the number of random start conformers. For the direct approach, n was chosen to produce the same number of accepted conformers as with a REDAC cycle and n=50. CPU times are given for a CRAY Y/MP (one-processor).

Example for DIANA results:

```
Result file of the program DIANA  (SGI version 2.8)


Input files:
Library                        : /scratch/huxley/diana-2.8-irix5/lib/diana.lib
Sequence                       : uuusugfix4.seq
Upper distance limits          : uuu6allmod.upl
Angle constraints              : uuu4.aco
Initial dihedral angles        : uuu4_f.ang

Number of residues             :      19
Number of atoms                :     639
Number of dihedral angles      :     207 (131 rotatable)
Number of stereospec. assignmts:       0 (0 %)
Number of upper distance limits:     220 (16 with special weight)
Number of lower distance limits:       0
Number of angle constraints    :      41
Number of structures           :      50
Number of minimization steps   :       3
Maximal number of iterations   :    6000
Cutoff for upper limits        :    0.20 A
Cutoff for lower limits        :    0.20 A
Cutoff for van der Waals limits:    0.20 A
Cutoff for angle constraints   :    5.00 deg
Cutoff for target fn. fraction :  100.00 %

Output files:
Overview                       : uuu4_g.ovw
Cartesian coordinates          : uuu4_g%%%.pdb

Minimization parameters (standard parameters):
    level |i-j|           weighting factors iter. vdw-update  funct. residue
    upl lol vdw  upper  lower     vdw  angle limit angle iter  cutoff range(s)
  1  19  19  19 1.0E+0 1.0E+0 2.0E-1A 5.0E+0  2000  10.0  100 1.0E+10 1..19
  2  19  19  19 1.0E+0 1.0E+0 6.0E-1A 5.0E+0  2000  10.0  100 1.0E+10 1..19
  3  19  19  19 1.0E+0 1.0E+0 2.0E+0A 5.0E+0  2000  10.0  100 1.0E+10 1..19

Structure   1: (random number generator seed: 467531)

Minimization:
   lev    upper    lower        vdw   angle target funct. |grad| #up   #f stop
          # act    # act     #  act   # act  begin    end    end
  1  0  134  57    0   0  1136    5  41   1 313.26   4.11 3.0E-3   0   83 gradtl
  2  1  193  88    0   0  4317   62  41   2 3.7E+3   3.78   0.10  48  400 flat
  3  7  197  88    0   0  4902  225  41   2 1.1E+4  11.74   5.26  20  463 flat
  4  9  202  89    0   0  5148  247  41   1 5.9E+3  12.67   4.29  10  445 flat
  5 11  205  94    0   0  5153  236  41   0 1.0E+4  13.59   5.18   8  306 flat
  6 13  211  89    0   0  5516  350  41   0 3.7E+3  23.95  14.07   6  248 flat
  7 15  215 104    0   0  5451  336  41   0 1.2E+3  27.09  14.59   7  320 flat
  8 17  220  99    0   0  5523  376  41   1 2.2E+4  29.19   8.63  12  602 flat
  9 19  220  99    0   0 12255  537  41   0  36.47  34.91  15.74   3  218 flat
 10 19  220 109    0   0 11843  409  41   0  85.62  65.72  36.41   9  778 flat
 11 19  220 109    0   0 11585  338  41   0 182.87 163.86  36.35   4  293 flat

Minimization:
   lev    upper    lower        vdw   angle target funct. |grad| #up   #f stop
          # act    # act     #  act   # act  begin    end    end
  1 19  220  95    0   0 10463  143  41   1   6.45   4.92   2.03   5  420 flat
  2 19  220  95    0   0 10353  109  41   1   6.74   6.07   7.62   3  202 flat
  3 19  220  96    0   0 10281   86  41   1   9.07   7.63  11.43   4  258 flat
...
Overview:

Number of accepted structures  :        50 (50 structures started)
Residue range for upper limits :        19
                  lower limits :        19
                  van der Waals:        19
Cutoff for upper limits        :      0.20 A
           lower limits        :      0.20 A
           van der Waals       :      0.20 A
           angle constraints   :      5.00 deg
CPU time                       :      6.71 min
CPU time per structure         :      0.13 min
```

```
Average number of iterations   :      1051

 struct   target   upper limits   lower limits  van der Waals   torsion angles
        function   #   sum  max   #   sum  max   #   sum  max   #    sum   max
  1  15     3.92  23  13.4 0.47   0   0.0 0.00   2   3.3 0.34   0    0.0   0.0
  2   3     5.73  31  14.8 0.55   0   0.0 0.00   4   4.1 0.39   0    1.0   0.9
  3  34     5.76  27  15.7 0.76   0   0.0 0.00   1   3.7 0.26   0    0.0   0.0
  4  31     5.99  31  15.4 0.53   0   0.0 0.00   5   5.7 0.38   1   14.7   6.8
  5  26     5.99  35  16.0 0.53   0   0.0 0.00   5   6.4 0.34   1    9.5   5.6
  6  29     6.18  30  14.6 0.79   0   0.0 0.00   5   5.1 0.61   0    0.0   0.0
Average    41.83  44  24.6 1.19   0   0.0 0.00  56  34.2 1.02   1   18.2  11.9
+/-        37.12  10   6.9 0.46   0   0.0 0.00  52  31.1 0.52   1   18.3  14.1
Minimum     3.92  23  13.4 0.47   0   0.0 0.00   1   3.3 0.26   0    0.0   0.0
Maximum   151.37  65  40.4 2.35   0   0.0 0.00 209 133.2 2.35   5   65.9  58.0

Constraint violation and hydrogen bond overview (structures ordered):

Cutoff for target function     :  1.00E+03
Number of structures included  :        50
Number of violated constraints :      1907
Number of consistent violations:         4
Maximal hydrogen bond length   :      2.40 A
Maximal hydrogen bond angle    :     35.00 deg
Number of hydrogen bonds       :       207
Number of consistent H-bonds   :         0
                                         max 1   5   10   15   20   25   30   35   40   45   50
Upper Q5’   RGUA   1 - H3’   RGUA   1   0.26   +  ++  +       ++ + ++  +  + +   *  +   ++   ++
Upper H1’   RGUA   1 - H8    RGUA   2   0.49   +++ +    ++++++ +     + ++ *           +    +  +
Upper H2’   RGUA   1 - H8    RGUA   2   0.49             *             +
Upper H3’   RGUA   1 - H8    RGUA   2   0.24                   +                              *
Upper H1’   RGUA   2 - H6    RCYT   3   0.93           +   +   +   +    +        +    ++++ +  *
Upper N2    RGUA   2 - O2    RCYT  18   0.33                                          *
Upper H1    RGUA   2 - H1’   RCYT   3   0.96                                     +     +     +*
Upper H1    RGUA   2 - Q4    RCYT  18   0.57                                          *
Upper H1    RGUA   2 - H1’   RCYT  19   0.89                                          *
VdW   OP1   RCYT  18 - O4’   RCYT  18   0.33            +                              *
VdW   H2’   RCYT  18 - O5’   RCYT  19   0.21                +                    +           *
VdW   O2’   RCYT  18 - C5’   RCYT  19   0.46                                          *
VdW   O2’   RCYT  18 - H5’   RCYT  19   0.53                                          *
VdW   HO2’  RCYT  18 - C3’   RCYT  18   0.39        +     +++*+          + +  +   +           +
Angle EPSI  RGUA   2                    5.73                                               *
Angle EPSI  RCYT   3                   58.01               +       +    +  +      *+  +
Angle EPSI  RGUA   4                   16.39            +                             *
Angle BETA  URA    5                    8.88            +                             *
Hbond H21   RGUA   2 - O2    RCYT  18     35 ++ + ++++++ +++++ + +  ++ ++  +  ++++++++  +++ +++
Hbond H21   RGUA   2 - N3    RCYT  18      8  + +  +      +  +         ++                +
Hbond H1    RGUA   2 - O4’   RGUA   4      1                                          +
Hbond H1    RGUA   2 - N3    RCYT  18     41 ++ ++++ +++++++++++ ++ ++ ++ +++++++ ++++ ++++ +++

Pairwise RMSDs (structures ordered):

Number of backbone atoms   :        72
Number of heavy atoms      :       258
Residues considered        :      2..7, 13..18
Local RMSD segment length  :         3 residues
Mean global backbone RMSD  :      5.07 +/- 2.41 A  (1.01..10.74 A)
Mean global heavy atom RMSD:      4.69 +/- 2.02 A  (0.99.. 9.45 A)

        1     2     3     4     5     6     7     8     9    10    11    12    13    14    15    16
  1    15  1.78  2.14  1.81  2.17  1.46  2.16  1.56  2.36  2.66  2.12  1.63  1.80  2.02  1.78  1.88
  2  1.58     3  1.24  1.71  2.10  1.53  1.49  2.37  3.61  3.63  3.15  2.25  2.80  2.31  2.10  1.73
  3  1.97  1.30    34  1.82  1.99  1.48  1.17  2.55  3.85  3.83  3.12  2.27  3.16  2.42  2.49  1.82
  4  1.75  1.73  1.71    31  1.82  1.51  2.37  1.87  3.21  3.41  2.49  2.23  2.60  1.99  2.22  1.06
  5  2.04  1.91  1.76  1.82    26  2.00  2.45  2.74  3.65  4.00  2.56  2.74  3.12  2.69  2.57  2.02
```

A newer program (DYANA, Güntert et al., 1997) employs a simulated annealing by molecular dynamics in the torsion angle space for the calculation of the solution structures. Because of the reduced number of degrees of freedom in torsion angle space compared to the carthesian coordinate space and because of the absence of high-frequency bond and angle vibrations the algorithm is faster. The target function (see above) serves as potential energy function in this torsion angle dynamics approach which also results in a slightly higher convergence of the calculations.

Appendix.

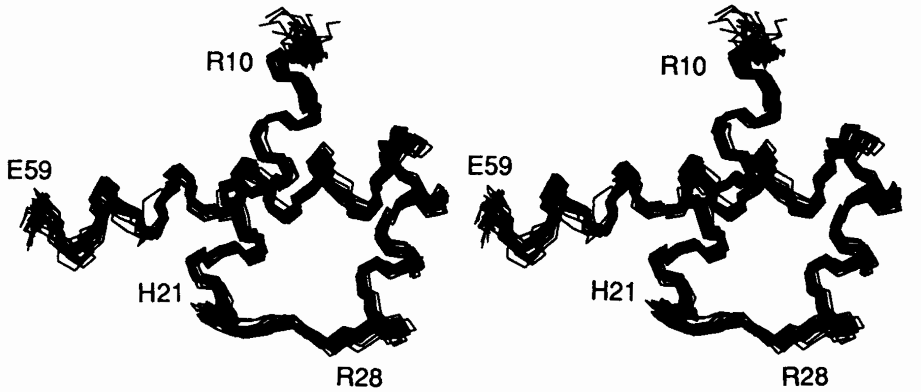

Stereo view of the superposition of the residues 7 to 59 of the 20 energy-minimized *Antp(C39 → S)* homeodomain structures The bonds connecting the backbone atoms N, C^α and C′ are shown.

Stereoview of 20 DIANA generated structures (Güntert et al., 1991).

Constraints defining the stereospecific assignments (Basus, 1989)

Conformation	g^2g^3	g^2t^3	t^2g^3
χ^1	60°	180°	- 60°
	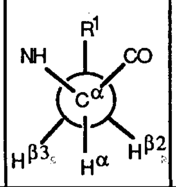	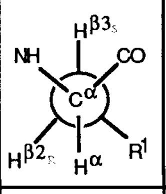	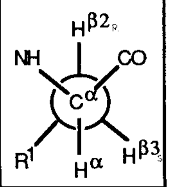
$^3J\alpha\beta^2$ (Hz)	2.6-5.1	2.6-5.1	11.8-14.0
$^3J\alpha\beta^3$ (Hz)	2.6-5.1	11.8-14.0	2.6-5.1
NOE(α,β^2)	Strong	Strong	Weak
NOE(α,β^3)	Strong	Weak	Strong
NOE(NH, β^2)	Weak	Strong-Medium	Strong
d(NH, β^2)(Å)	3.5-4.0	2.5-3.4	2.2-3.1
NOE(NH, β^3)	Strong-Medium	Strong	Weak
d(NH, β^3)(Å)	2.5-3.4	2.2-3.1	3.5-4.0

References:

Conventions, proteins: JBCN, Biochemistry (1970) 9/18, 3471-3479
Conventions, nucleic acids: JBCN, Eur.J.Biochem. (1983) 131, 9-15
Pseudo atoms: Wüthrich et al., J.Mol.Biol. (1983) 169, 949-961
Structure calculation:
Crippen, J.Comp.Phys. (1977) 24, 96-107
Havel et al., Bull.Math.Biol. (1983) 45, 665-720
Braun & Go, J.Mol.Biol. (1985)186, 611-626
Güntert et al., J.Mol.Biol. (1991) 217, 531-540
Güntert & Wüthrich, J.Biomol.NMR (1991) 1, 447-456
Güntert et al., J.Mol.Biol. (1997) 273, 283-298
Wishart & Sykes, J.Biomol.NMR (1994) 4, 171-180
Basus, Methods Enzymol. (1989) 177, 132-49

Perutz, Protein structure, Freeman & Co., New York, 1992
Creighton, Proteins, Freeman & Co., New York, 1984
Fasman, Prediction of protein structure and the principles of protein conformation, Plenum Press, New York, 1989
Saenger, 1983, Principles of nucleic acid structure, Springer, Berlin, 1984
Neuhaus & Williamson, The nuclear overhauser effect, VCH, Weinheim, 1989
Roberts, NMR of Macromolecules, Oxford University Press, Oxford, 1993